International Journal of Inventive Engineering and Sciences (IJIES)
ISSN: 2319-9598 (Online), Volume-12 Issue-12, December 2025

Integrated Petrophysical Evaluation and Reservoir Characterization of the Zarama Field, Offshore Niger Delta using Multi-Well Geophysical Log Analysis

Mohammed Ali Garba, Mustapha Ali Garba

Abstract: ***The paper will provide a detailed petrophysical study of the Zarama field in the Niger Delta, based on wireline logs from five wells. Porosity, permeability, shale content, and fluid saturations are the primary reservoir parameters in the study, used to analyse reservoir quality, heterogeneity, and producibility. Porosity is good to excellent (20-32 per cent), declining with depth in response to compaction, and quite diverse (7-781 mD), primarily determined by shale volume, not by its porosity. Reservoir thickness ranges from 6 m to more than 700 m, and lateral continuity has been found in the massive sands such as S1, S3, S14, and S16, which contain large hydrocarbon pore volumes and have high production potential. The solution of fluid contacts (gas-water, gas-oil, oil-water) was possible even in the absence of a density log anomaly due to the presence of gases. The field is rather gas-bearing, with minor quantities of oil and condensate. It thus has an estimated recoverable reserve of 2.85 million barrels of oil equivalent and 5.85 billion cubic feet of gas. Multi-well and multi-reservoir system petrophysical interwell correlations show no clear stratigraphic trap system, and these demands require integrated multi-well, multi-reservoir system interpretation to obtain adequate characterisation of the reservoir and development planning. All in all, the research indicates that integrated log interpretation improves dataset reliability, optimises petrophysical parameters with high confidence, and provides a robust framework for future exploration and development in this complex offshore deltaic setting.***

Keywords: Wireline Logs, Porosity, Permeability, Shale Content, Heterogeneity, and Producibility

Nomenclature:
Md: Millidarcy unit of Permeability
Vsh: Volume of Shale
G: Gamma Ray Reading in the Zone of Interest
G_{cs}: Gamma Ray Reading in Clean Sand and
G_{sh}: Gamma Ray Reading in Shale Zones
SPDC: Shell Petroleum Development Company
RR: Recovery Factor

Manuscript received on 06 December 2025 | Revised Manuscript received on 12 December 2025 | Manuscript Accepted on 15 December 2025 | Manuscript published on 30 December 2025.
*Correspondence Author(s)
Mohammed Ali Garba*, Department of Geology, Gombe State University, Gombe, Nigeria. Email ID: mohammedaligarba@gsu.edu.ng, ORCID ID: 0000-0001-6247-8702
Mustapha Ali Garba, Department of Physics, University of Maiduguri. Nigeria. Email ID: mustaphaaligarba@gmail.com, ORCID ID: 0009-0004-9655-0855

© The Authors. Published by Blue Eyes Intelligence Engineering and Sciences Publication (BEIESP). This is an open-access article under the CC-BY-NC-ND license http://creativecommons.org/licenses/by-nc-nd/4.0/

I. INTRODUCTION

A. Highlights

- The Wells 1 to 5 reservoirs have good to excellent values of porosity, with roughly 20% to 32% porosity, and the porosity of the reservoirs declines with depth, resulting in the compaction effect. Despite this comparably steady porosity, permeability is very variable-again, typically determined by Vsh, not by porosity alone-with permeability values ranging down to 7 millidarcies (mD) in some sands and more than 780 mD in other sands. Permeable sands such as S1 are consistently highly porous and have strong hydrocarbon potential.
- Sixteen reservoirs (S1-S16) were defined, and this was laterally non-uniform, showing an example of lateral heterogeneity in a deltaic depositional system. In this case, sample, depositional variability, or a change in sediment supply results in some reservoirs not forming in some wells, i.e., the reservoirs have been pinched out. However, thick, laterally continuous sands (with good reservoir characteristics) such as S1, S3, S14, and S16 indicate potential areas, particularly in the deep offshore sections of the field.
- Combined log evaluations depict the field to be primarily gas-charged as indicated by high resistivity and neutron-density cross-overs. Data gaps were addressed by delineating fluid contacts, such as gas-water, gas-oil, oil-water, and shale contacts. There are also instances of oil and condensate charges. The availability of thick shale sealing units and stratigraphic traps promotes hydrocarbon entrapment and the field's producibility.
- The evident petrophysical variability and heterogeneity lead to the need to apply the integrated multi-well-log analysis aimed at describing the architecture of the reservoir, fluid distribution, and reserves that can be produced. Porosity, permeability, shale volume, and fluid saturations are correlated, ensuring reliable reserve estimation and development planning in this intricate Niger Delta deltaic scenario. This integration helps reduce the difficulties caused by data gaps or inconsistencies and supports sound field development approaches.

Cluster analysis, geostatistics, estimations of reservoir quality as part of

© Copyright: All rights reserved.

defining complex, clastic reservoirs, and dynamic simulation. The technique enhanced knowledge of the reservoir's heterogeneity and flow dynamics by classifying flow units and plotting their spatial characteristics. The models were able to fit historical data, which provided helpful information on production performance and enabled more effective reservoir management [1]. These sensors record data, which is sent to surface equipment through a steel-armoured electrical cable, and the data are processed and presented as continuous well logs that indicate variations in properties such as spontaneous potential, resistivity, or density with depth. These measurements allow the calculation and maximisation of hydrocarbons that can be produced [2]. The Zagros structures have average porosities of 12 and 10, which remain economically recoverable. The water saturation model based on the application of the Indonesia equation was effective in complex environments and aided in interpreting fluid distributions. Multi-mineral models were tailored to increase mineral estimates, and porosity-permeability relationships were based on empirical data to improve reservoir evaluation. The validity of the models was checked using calibration with core data. To reinforce results, the datasets should be enhanced and sophisticated logging should be implemented. On balance, the research contributes to knowledge of the reservoir and proposes maximising hydrocarbon recovery [3].

The Niger Delta Basin along the south African coast of Nigeria was studied by integrating three methods of analysis, including well log analysis, seismic interpretation, and petrophysical evaluation, to define four reservoir intervals (A-D) in four wells oriented southwest to northeast. Findings indicated a decrease in reservoir quality to the southwest, where well B10 is located, and to the northeast, where resistivity responses show decreasing values, indicating a reduction in reservoir potential. This was supported by seismic mapping, which revealed a southward dip in the bottom beds of the reservoir and structurally high updip positions at B10 and B2, and B3 ST1 drilled lower and downdip areas. The petrophysical data showed that the reservoirs are not yet fully exploited, and the reservoir trapping is likely both structural and stratigraphic, given lithological variations. It is important to note that clues of gas-water contact and incomplete reservoir fill imply that the reservoir was near-complicated in nature, and these findings are helpful for future exploration and development plans in the area [4].

The significant advancements in petrophysical modelling of the Zagros region have integrated diverse datasets and employed probabilistic methods to understand reservoir heterogeneity better. However, a notable research gap remains in the limited availability and comprehensiveness of datasets, especially regarding shale content and geological complexity, which hampers the generalizability and accuracy of reservoir characterization [5]. The comprehensive understanding of petrophysical properties in the Sapphire wells, particularly regarding the variability in porosity, permeability, and shale content derived from gamma-ray and neutron logs. Despite detailed lithological and reservoir classifications, limited data on the spatial heterogeneity of these properties and their influence on fluid flow and hydrocarbon potential hinder accurate reservoir characterization and development planning [6].

[7] Demonstrates that integrating advanced well-log interpretation with geological and petrophysical data significantly improves the accuracy of reservoir characterization and hydrocarbon assessment. Despite extensive use of well-log interpretation for reservoir evaluation and petrophysical characterization, a significant research gap remains in developing integrated, advanced models that accurately incorporate geological, geophysical, and petrophysical data to address uncertainties in complex reservoirs. Current methodologies often struggle to fully account for heterogeneity, fluid effects, and data inconsistencies, leading to inaccuracies in estimating reservoir quality and hydrocarbon potential. An example of petrophysical analysis of five wells in the Niger Delta to describe six reservoirs, in terms of their thickness, shale volume, porosity, and water saturation. The trusted information and research were critical to determining hydrocarbon zones, reservoir management, and the viability of the reservoirs for hydrocarbon extraction [8].

Geophysical well logging is a crucial tool for exploring and assessing hydrocarbon reservoirs. Well logs generate detailed, continuous data on the lithology of rocks, porosity, fluid content, and reservoir quality by estimating several physical properties of subsurface formations, including resistivity, density, neutron porosity, and acoustic transit time. These results are essential in identifying the presence or producibility of hydrocarbons within a field. The Niger Delta is one of the most prolific hydrocarbon basins in Africa, with complex stratigraphy comprising sand to shale beds, mainly of the Agbada Formation. Gathering the idea about the petrophysical properties of these rocks: Porosity, permeability, saturation levels of water, and the volume percentage of shale, is essential to characterize the reservoir effectively and extract the maximum number of hydrocarbons. This is a paper on the Zarama field in the Niger Delta, where they use 5 wells as a case study to analyse well logs and develop key reservoir parameters. The investigation aims to differentiate the reservoir units, determine approximate fluid saturations, and evaluate reservoir quality by integrating various logging measurements. In addition, the paper assesses fluid contacts. It estimates recoverable reserves, providing a clear indication of the field's production potential and where future development should be focused. Although comprehensive petrophysical reviews of the Zarama field have been carried out, several challenges and limitations have affected data analysis and interpretation. Another problem was the presence of unreliable density logs, especially in Well-1, where density measurements in shallow intervals showed unrealistic results (up to 100 g/cc) likely due to gas or a tool calibration error. Such anomalies required specific data; in some cases, only resistivity logs were used,

Published By:
Blue Eyes Intelligence Engineering and Sciences Publication (BEIESP)
© Copyright: All rights reserved.

which could conceivably add ambiguity to estimates of porosity and fluid saturation. The other weakness was that some details of log coverage were left uncovered in certain wells, such as gamma situations or neutrons used in Wells 3 and 4, with lithology and porosity adjustments having insufficient confidence in such areas.

Also, deep lithological stratigraphic heterogeneity, finely stratified sands, and lateral discontinuity between wells, when found, hampered the correlation of reservoir units and the mapping of fluid contacts that could affect volumetric calculations of reserves. The interpretation of fluid type using neutron-density crossovers and resistivity also posed difficulties in differentiating gas and oil, or water, in zones where logs were shifted due to borehole conditions or invasion effects. In addition, there is a lack of core data to directly calibrate petrophysical parameters, thereby impeding validation of the logging datum; however, region analogues were used to provide a point of calibration. Broadly adopted empirical equations used to estimate permeability inherently rely on this supposition based on average grain size and sorting; they may not adequately describe the entire range of reservoir quality throughout the field. Future research and development will need to address reservoir characterisation by integrating solutions such as higher-resolution log acquisition, core analysis, and advanced petrophysical modelling to minimise uncertainties and enhance the accuracy of reservoir characterisation. Petrophysical analysis of the Zarama field in the Niger Delta was based on well logs from five wells, and the interpretation of gamma ray, resistivity, density, and neutron logs was a factor in specifying the reservoir characteristics.

II. METHOD AND MATERIALS

To conduct a logging operation, a probe or sonde is lowered into the well on an insulated electrical cable, which supplies power and transmits sensor data back to the surface. Depth is measured via the cable. Data is processed and plotted both analogously and digitally. While most logs are recorded during pull-out, some methods, such as MWD, LWD, and flow-meter logging, are recorded during descent. Logging tools include gamma ray, resistivity, density, neutron, and sonic, among others.

A. Resistivity Logging: Evaluation of fluid content in oil and water wells uses electrical resistivity to identify water or hydrocarbons by measuring ion flow through pore fluids. Higher resistivity suggests better water quality or higher hydrocarbon content, while lower values indicate saline water. Resistivity at different depths, obtained by varying electrode spacing, helps detect invasion zones and permeability, which are influenced by factors such as salt concentration, temperature, and porosity.

Where Ra is the resistivity of a 100 percent water-filled formation, and Rw is the resistivity of the water.

Formation Resistivity Factor: Formation Resistivity Factor (F), the ratio of resistivity in a fully water-saturated formation (Ra) to that of formation water (Rw), aids interpretation of measurements. Electric logging tools apply voltage between electrodes, causing current flow in formation fluids. The resulting voltage reflects formation resistivity, with electrode spacing determining investigation depth. Short- and long-spacing data provide shallow and deep resistivity data, which are vital for evaluating reservoir fluid type, characteristics, and permeability for exploration and production.

B. Acoustic Logging: An Acoustic Log, or sonic log, provides valuable information on the physical structure of rock matrices using tools such as the long-spacing sonic tool, a slender version for tubing installations, and the borehole-compensated tool. These instruments consist of transmitter and receiver transducers that convert electrical energy to mechanical energy and vice versa. The borehole-compensated tool measures two at values from multiple receivers and averages them to eliminate errors caused by sonde tilt and borehole size variations. Since transit time includes borehole fluid and formation travel, acoustic logs reveal transit time (density) and amplitude (interconnections) and also demonstrate that at relates to porosity and that the bulk velocity (Vb) is defined as the sum of fluid and matrix velocities, with the relation between bulk velocity (Vb) and fluid velocity (Vf) described by Willy's equation.

$$F = \frac{R_0}{R_w} \quad \ldots \quad (1)$$

Where Ra is the resistivity of a 100 percent water-filled formation, and Rw is the resistivity of the water.

Formation Resistivity Factor: Formation Resistivity Factor (F), the ratio of resistivity in a fully water-saturated formation (Ra) to that of formation water (Rw), aids interpretation of measurements. Electric logging tools apply voltage between electrodes, causing current flow in formation fluids. The resulting voltage reflects formation resistivity, with electrode spacing determining investigation depth. Short- and long-spacing data provide shallow and deep resistivity data, which are vital for evaluating reservoir fluid type, characteristics, and permeability for exploration and production.

C. Acoustic Logging: An Acoustic Log, or sonic log, provides valuable information on the physical structure of rock matrices using tools such as the long-spacing sonic tool, a slender version for tubing installations, and the borehole-compensated tool. These instruments consist of transmitter and receiver transducers that convert electrical energy to mechanical energy and vice versa. The borehole-compensated tool measures two at values from multiple receivers and averages them to eliminate errors caused by sonde tilt and borehole size variations. Since transit time includes borehole fluid and formation travel, acoustic logs reveal transit time (density) and amplitude (interconnections) and also demonstrate that at relates to porosity and that the bulk velocity (Vb) is defined as the sum of fluid and matrix velocities, with the relation between bulk velocity (Vb) and fluid velocity (Vf) described by Willy's equation.

Published By:
Blue Eyes Intelligence Engineering and Sciences Publication (BEIESP)
© Copyright: All rights reserved.

$$\frac{1}{V_b}=\frac{f}{V_r}+\frac{1-f}{V_{ma}} \quad \ldots \quad (2)$$

The equation for porosity (Θ) obtained from transit time (Δt) (which is the reciprocal of velocity) is:

$$\theta=\frac{\Delta t_{log}-\Delta t_{ma}}{\Delta t_f-\Delta t_{ma}} \quad \ldots \quad (3)$$

Where Δt_{log} = measured transit time, Δt_f = fluid time transit, and Δt_{ma} = assumed matrix transit time.

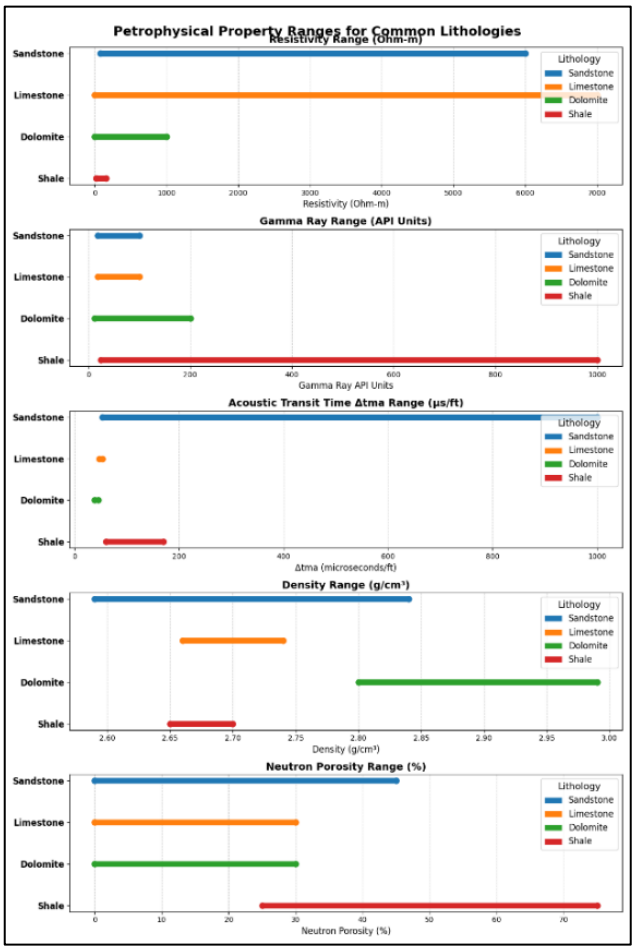

[Fig.1: Petrophysical Property Ranges for Common Lithologies]

D. Neutron Logging: A neutron log measures formation porosity around a borehole by detecting hydrogen atoms via gamma rays emitted when high-energy neutrons, from sources like Plutonium or Beryllium, collide with hydrogen nuclei and lose energy. Thermalised neutrons are captured by nuclei, which emit detectable gamma rays. A high hydrogen concentration near the borehole traps neutrons, resulting in lower gamma counts indicative of high porosity. In contrast, low-hydrogen areas allow neutrons to travel farther, generating higher counts and lower porosity. Non-porous, dense rocks (e.g., limestone) show high counts, while shale, rich in bound water, has low counts despite low porosity, complicating lithology interpretation without supporting logs. Neutron logs function in various borehole fluids, aid correlation with gamma-ray or casing-locator logs, and detect the presence and movement of gas due to hydrogen density changes, making them valuable for production logging and fluid dynamics analysis.

E. Density Logging: Density logging tools measure the bulk density of formations within a wellbore using a dense metal mandrel that collimates backscattered gamma rays. A calliper ensures proximity to the wellbore wall, enabling accurate measurements. The instrument includes a scintillation detector, typically a sodium iodide crystal, which converts gamma rays into light photons, which are then converted into electrons within a photomultiplier tube. These electrons are amplified through dynodes, producing pulses proportional to the detected gamma rays. Analysis of these signals yields the formation bulk density, which is essential for determining porosity and lithology. Well logging in oil and gas exploration entails measuring the physical properties of underground formations, which in most cases may necessitate casing the wells. Through-casing acoustic logging is susceptible to casing-wave interference, particularly when bonding is poor. To address this, an acoustic tool with dual sources was developed, incorporating an additional transducer to eliminate casing waves. The design of the tool includes designated distances between the transmitters and receivers and a dual-source transmitting circuit that produces signals with opposite polarity, thus cancelling out the casing waves. Chinese cased well testing revealed an approximately 90 per cent reduction in casing-wave amplitudes and enabled increased formation data to be recorded. Nevertheless, total cancellation is hindered by mechanisms such as propagation-path differences, random cement bond, frequency dispersion, and minor variations in transducer parameters. Nonetheless, these obstacles do not impede the fact that the suppressed casing waves can be used to achieve a better signal quality; thus, through-casing acoustic logging is a viable technique to get reliable data about the subsurface formations [9].

$$\delta_e=\delta_b(2\frac{Z}{A}) \quad \ldots \quad (4)$$

where σ = bulk density, o = electron density, Z-sum of the electrons, A total atomic weight

Table I: The Z/A Ratios for Sandstone, Limestone, and Dolomite Are

Rock Type	Z/A Ratio
Sandstone: (SiO2)	Z/A=0.499
Limestone: (CaCO3)	Z/A=0.500
Dolomite: (CaMg(CO3)2)	Z/A-0.499

In borehole measurements, acoustic logging is used to determine the velocity of sound waves in geological formations by primarily measuring the first-arrival times of compression waves. It was initially a high-resolution instrument designed to measure the interval of these waves using a transmitter and two closely spaced receivers, which provide high-resolution information on formation velocities,

Published By:
Blue Eyes Intelligence Engineering and Sciences Publication (BEIESP)
© Copyright: All rights reserved.

lithology, fracturing, and other properties. In deviated or horizontal wells, acoustic logging provides better lateral resolution than vertical resolution and is therefore helpful for characterising formations, assessing cementation, porosity, permeability, and microseismic activity [10]. The technique involves using water-filled wells, low logging rates, and proper tool positioning, while accounting for casing conditions and well stability to ensure accurate measurements. They revealed that formation bulk density had a direct correlation with porosity (0), fluid density, and matrix density of the rock material, with bulk density (a) being the fluid density (a) of the pore space plus the density of the matrix (Gm) (Table 1 and 2) [11].

$$\delta_b = \phi.\ \delta_f + (1\text{-}\phi).\ \delta_{mn} \quad \ldots \quad (5)$$

Rearranging the equation,

$$\Phi = \frac{\sigma_{ma}\text{-}\sigma_b}{\sigma_{ma}\text{-}\sigma_f} \quad \ldots \quad (6)$$

Porosity (0) can be calculated given bulk density (os), and if fluid density (or) and
matrix density (...) are known. The densities of some lithologies are shown in Table 1.
Typical fluid density (ρd) of water is 1.0 g/cc. Formation fluids containing oil and gas 0.7
g/cc. Formation fluids containing gas 0.3 g/cc.

Table II: Densities of Typical Lithologies [11]

Lithology	Range (g/cm³)	Matrix (g/cm³)
Clay-shales	1.8 - 2.75	Varies (Ave. 2.65-2.7)
Sandstone	1.9 – 2.65	2.65
Limestone	2.2 – 2.71	2.71
Dolomites	2.3 – 2.87	2.87

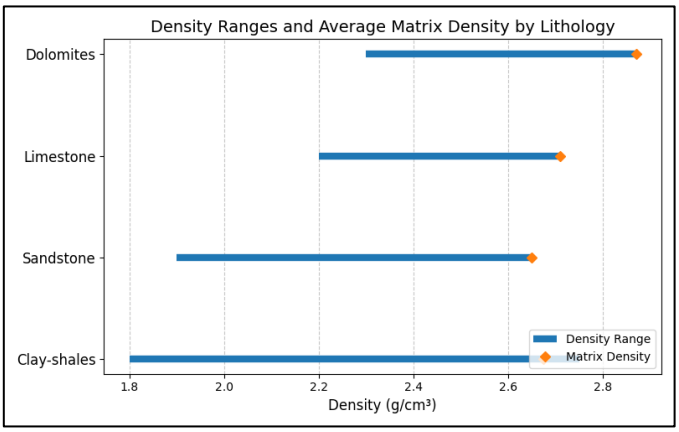

[Fig.2: Densities of Typical Lithologies]

F. Gamma Ray Logging: The natural gamma radiation in rock formations is varied because it contains radioactive minerals, including Uranium, Thorium, and Potassium, which are associated with specific depositional environments. Sedimentary sandstones and carbonates tend to have low gamma radiation, with clay and shale formations having high gamma radiation content. The count of gamma-ray logs in counts or API units helps determine lithology, with clean sands recording low counts and shaly formations having high counts [12]. An increase in gamma is associated with more compacted formations with lower porosity and permeability, and greater clay content. The writer observed that structures with many gammas tend to be less preferable for oil and water production, even though the surface water saturation may be low ([13]). The gamma-ray instrument employs a scintillator, typically a sodium iodide crystal, which produces an electrical pulse proportional to the gamma-ray energy deposited after a collision. In addition to determining shale occurrence intervals, gamma ray logs assess shale volume, an essential parameter for ensuring that other log measurements are corrected for shale-clay effects during reservoir assessment.

III. DATA ANALYSIS

The data set for this study comprises geophysical logs—including gamma ray, resistivity, density, and neutron logs—collected from five wells within the Zarama field, supplied by Shell Petroleum Development Company of Nigeria Limited (SPDC) in Port Harcourt, Nigeria. These logs were obtained using standard wireline logging methods, with density, neutron, and gamma-ray measurements recorded by a single tool and resistivity acquired by a separate instrument. Reservoir petrophysics involves measuring well data, processing it, and integrating these results into physical models that describe the reservoir rock at both the well and field scales. This includes calculating and interpreting key reservoir properties and correlating them with data from core samples, tests, and production to characterize the reservoir accurately. According to [14], the petrophysical characteristics of the Yagesiemu Formation in Tarim Basin, which has been found to have effective porosities between 7 and 10 percent, permeabilities ranging between 3 and 8.6 mD, and a gas saturation of 40 to 57 percent. The southwestern and northwestern areas are favourable for hydrocarbons, and the lithology is predominantly laminated shale and sandstone. The results help interpret reservoir variability for future exploration. Essential petrophysical properties for assessing hydrocarbon producibility are porosity, permeability, and water saturation (Sw), the fraction of pore space filled with formation water. Porosity fully saturated with water (Sw = 100%) is not viable for oil production, linking Sw to bulk-volume water (B), the percentage of total formation volume made up of water, by:

$$B_{vw} = \phi S_w \quad \ldots \quad (7)$$

Given the critical importance of the S, as discussed above, many techniques have been proposed for determining its value for a given formation. In log interpretation, the standard approach to water saturation is through the Archie formation factor process, defined by

$$F = \frac{R_0}{R_w} = \frac{C_w}{C_0} \quad \ldots \quad (8)$$

Published By:
Blue Eyes Intelligence Engineering and Sciences Publication (BEIESP)
© Copyright: All rights reserved.

The resistivity of a reservoir rock fully saturated with an aqueous electrolyte is related to the electrolyte's resistivity, with their corresponding conductivities linked accordingly. Using porosity (φ) and resistivity (R), Archie's formation factor analysis provides empirical relationships connecting porosity to formation factor and resistivity to water saturation (S). Petrophysical information for the Zarama field is limited, so this study uses well-log data to evaluate reservoir productivity and estimate reserves. Wireline logs from five wells reveal the Agbada Formation's alternating sand and shale sequences, with key reservoir properties like porosity (20–32%), permeability (7–781 mD), and shale volume derived from gamma-ray, resistivity, density, and neutron logs. Fluid contacts such as gas-water and oil-water were identified, with gas predominating. Despite challenges such as inconsistent density logs in gas zones, integrated log analysis enabled reliable mapping of reservoir heterogeneity, thickness variations, fluid saturations, and promising recoverable reserves due to well-developed hydrocarbon traps (Fig. 3).

Table III: Resistivity, Gamma Ray, Transit Time, Density, and Neutron Value of Different Materials

	Material	Resistivity (Ohm-m)	Gamma Ray API API$^{(o)}$	Δtma	Density (g/cm^3) (ma)	Neutron Porosity
Common Lithology	Sandstone	Top 1000	18 – 160	53 - 1000	2.59 -2.84	0 – 45
	Limestone	80-6 X 10^3	18 – 100	47.6 - 53	2.66 – 2.74	0 – 30
	Dolomite	1-7 X 10^3	12 - 200	38.5 – 45	2.8 -2.99	00 -3-
	Shale	0.5 - 1000	24 - 1000	60 -170	2.65 – 2.7	25 - 75
Matrix Minerals	Quartz	10^4 - 10^{12}	0	51.2 – 56.0	2.64 – 2.65	-2
	Calcite	10^2 - 10^{12}	0	45.5 -49.0	2.71	-1
	Dolomite	1-7 X 10^3	0	38.5 – 45.0	2.85 -2.88	1
Clay Minerals	Illite	-------	250 - 300	-----	2.52 – 3.00	30
	Chlorite	-------	180 – 250	-----	2.60 -3.22	52
	Kaolinite	-------	50 – 130	-----	2.40 – 2.69	37
	Smecrite	-------	150 -200	-----	2.00 – 3.00	44
Micas	Glauconite		75 - 90	-----	2.2 – 2.8	38
	Muscovite	10^{-11} - 10^{12}	140 -270	49	2.76 -3.1	20
	Biotite	10^{18} - 10^{23}	90 -275	50.8 – 51	2.65 – 3.1	21
Feldspar Minerals	Microcline	-----	220 -280	45	2.53 – 2.57	30
	Orthoclase	-----	220 - 280	69	2.52 -2.63	30
Coals	Anthracite	10^{-9} - 10^{23}	0	90 - 120	1.32 – 1.80	38
	Bituminous coal	10 - 10^2	0 – 18	100 - 140	1.15 – 1.7	60
	Lignite	4 - 10^3	6 - 24	140 -180	0.5 – 1.5	52
Fluids/Gas	Gas	ά	0	-----	0.000386	-----
	Methane	ά	0	626	0.00076	-----
	Oil (40^4) API	10^7 - 10^{14}	0.12 – 0.40	238	0.85 – 0.97	60
	Pure water	ά	0	189 - 207	1.00	100
	Salt water (33.00 ppm)	0.031	0	180	1.19	60
Metallic Minerals	Pyrite	10^{-4} - 10^{-2}	-----	39.2 -39	4.8 – 5.17	-3
	Siderite	10^2 - 1000	0	47	3.0 – 3.89	12
Evaporites	Halite	<10^2 - 101^4	0	66.7 - 67	2.03 – 2.08	-3
	Anhydrite	10^2 - 10^{14}	0 – 12	50	2.89 – 3.05	-2
	Gypsum	1000	0	52 - 53	2.33 – 2.40	60
	Sylvite	10^{20} - 10^{24}	500	74	1.86 – 1.99	-3
	Polyhalites	-----	200	57.5 - 58	2.79	25
Crystalline Rocks	Basalt	6 x 10^2 - 10^4	12 - 24	45 – 57.5	2.7 – 3.2	-----
	Granite	10^6	24 - 96	46.8 – 53.5	2.52 – 2.8	-----
	Gneiss	10^2 - 10^6	24 - 48	48.8 – 51.6	2.6 -3.04	-----

© Copyright: All rights reserved.

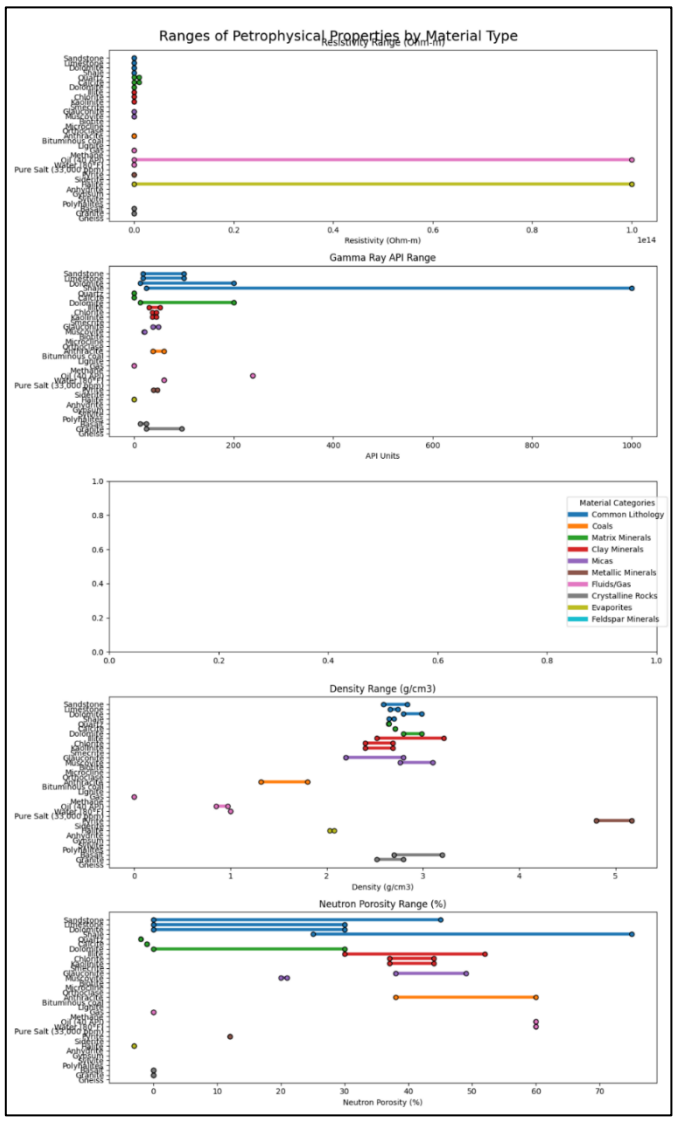

[Fig.3: Resistivity, Gamma Ray, Transit Time, Density, and Neutron Value of Different Materials]

A. Petrophysical Data Analysis

The obtained raw data were plotted into well log signatures using an Excel spreadsheet on a linear scale (gamma ray, density, and neutron logs) and a logarithmic scale (resistivity log) for each of the five wells, with the gamma-ray log on track 1 and resistivity, density, or neutron logs on tracks 2 and 3 for the same depth. In wells 1 and 5, the resistivity log was placed on track 1 for the absence of gamma-ray log and density and/or neutron logs on tracks 2 and 3 as applicable.

i. *Shale Volume:* Green Field in the Niger Delta contains low shale content, high sand content, and good permeability, indicating the potential for significant hydrocarbons. Oil is in reservoirs; there is no gas, and there will be minimal shale intercalations, unlikely to cause hindrance. The Steiber technique is the most valid when estimating the shale. In general, the field has future potential for exploration and development, and the following relationships were used [15]

The parameter also served as input data in the porosity and saturation model for shaly sand.

$$V_{sh} = 0.33(2^{2.1\,GR}) - 1.0) \quad \ldots \quad (9)$$

where V_{sh} = shale volume

$$\text{and } I_{GR} = \frac{G - G_{cs}}{G_{sh} - G_{cs}} \quad \ldots \quad (10)$$

G = gamma ray reading in the zone of interest
G_{cs} = gamma ray reading in clean sand and
G_{sh} = gamma ray reading in shale zones.

[16] The shale volume (Vsh) plays a vital role in reservoir analysis and was estimated using various methods across five wells. The linear Gamma Ray gave the highest values, and the Neutron-Density the lowest, although the non-linear Gamma Ray (Larionov) gave more consistent and reliable results. The estimation of Vsh in this field is recommended to be done using the non-linear Gamma Ray method, as the Neutron-Density method is challenging to apply due to logging problems. In wells 1 and 5, shale volumes, Vsh, were computed using the expression:

$$V_{sh} = \frac{\left[\frac{R_{sh}(R_{cs} - R_t)}{R_t(R_{msh} - R_{sh})}\right] 1}{2} \quad \ldots \quad (11)$$

Where R_{sh} is the resistivity of 100% shale formation, R_{cs} is the resistivity of clean sand, R_t is true resistivity, and R_{msh} is the maximum resistivity in the shale pay interval.

ii. *Porosity:* Reservoir porosities were computed from density logs using the expression after [17].

$$\phi_d = \frac{\rho_m - \rho_b}{\rho_m - \rho_r} \quad \ldots \quad (12)$$

Neutron porosities (0) were read directly from neutron logs. The porosities were corrected for shale using the expression [17].

$$\phi_d = \frac{\rho_m - \rho_b}{\rho_m - \rho_r} - \frac{\rho_m - \rho_b}{\rho_m - \rho_{sh}} V_{sh} \quad \ldots \quad (13)$$

Where p is the density of adjacent shale

The porosities from density and neutron logs in well 5 were integrated to obtain equivalent porosities (0) using [17] relations:

$$\phi_e = \sqrt{\frac{\phi_n^2 + \phi_d^2}{2}} \quad \ldots \quad (14)$$

Formation resistivity factor (F) was determined using the equation.

$$F = \frac{1}{\phi^m} \quad \ldots \quad (15)$$

Where a is the cementation constant, and m is the cementation factor. Cementation constant a=1 was used in this study, and the cementation factor m was

Published By:
Blue Eyes Intelligence Engineering and Sciences Publication (BEIESP)
© Copyright: All rights reserved.

reported by [18] to be 1.8. The value of m 1.8 was used in this study.

iii. Water and Hydrocarbon Saturations: Calculating water saturation (Sw) is challenging because various approaches yield different results, which can dramatically affect hydrocarbon volume estimates. The need to resolve these differences and properly map Sw is critical, and the uncertainties in the transition zones typically range from -5% to +15%. Beyond the transition zones, uncertainties are reduced to around 3%-10%. Water and hydrocarbon saturations are usually estimated from well logs [19]. saturation equation.

$$\frac{S_w = \left[\frac{R_0}{R_t}\right] 1}{2} \quad \ldots \quad (16)$$

$$S_h = 1 - S_w \quad \ldots \quad (17)$$

where S_w is water saturation
R_0 = resistivity of 100% water-filled formation
R_t = true resistivity
n = saturation exponent
S_h hydrocarbon saturation
Reformation water resistivity

A saturation exponent of n = 2 was used in this study. Mature oil field development is becoming increasingly significant and entails high-level reservoir management, particularly tertiary recovery techniques such as gas, chemical, and thermal injections. The main issues are identifying residual oil, selecting appropriate methods, and planning long-term actions amid economic uncertainty. Although tertiary techniques typically recover only a small percentage of the oil initially, they may increase ultimate recovery in large or long-life fields, and timing and efficiency are key to success. In general, the process of mature field development needs to be optimised and strategised, with specific consideration of each field. However, R could not be directly determined from the available deep resistivity logs, so [20]

Relations for water saturation, S., were used as follows.

$$S_w = \left[\frac{R_{ns}.10^{Yt}}{R_t}\right] 1/n = \left[\frac{R_{ns}.10^{Yt}}{R_t}\right] 1/2 \quad \ldots \quad (18)$$

Where. $10^{Yt} = R_0$ *and* R_{ns} is the resistivity of non-source shale and Y_t

Is defined by

$$Y_t = log_{10}\left[\frac{R}{R_{ns}}\right] \quad \ldots \quad (19)$$

iv. Permeability: Permeability was estimated from porosity and Vsh using the formula:

$$K = 10^{[A + B\,log(\phi) + C\,V}sh \quad \ldots \quad (20)$$

Where A, B, and C are constants defined as follows:
A = 7.432; B=8.060; and C = -5.508

Clays and shales have low, hard-to-define permeability, particularly at large scales where fractures and faults can significantly affect flow. Existing models, such as Darcy's, may not capture all flow in such materials due to non-Darcian and coupled processes, such as chemical osmosis. These doubts complicate the use of applications such as waste disposal and basin pressure analysis, and developments increasingly depend on advanced molecular simulations to understand flow at the pore scale. This equation accounts for grain size and sorting through the Vsh (shale content) term, and grain size and sorting significantly affect permeability [21]. From the petrophysical properties and/or parameters evaluated from the well logs from each of the wells, reservoir components- water, oil, and gas were identified, and their contacts (gas-oil-contact- GOC; oil-water-contact-OWC; gas-water-contact-GWC; gas-down-to-shale-GDT; and oil-down-to-shale-ODT) were established and net pay computed.

v. Reserve Estimate: Hydrocarbon pore volume (HCPV) under reservoir conditions was estimated empirically as a function of reservoir rock and fluid properties, following the [22] standard volumetric equation.

$$HCPV = AHNGx\theta xS_h \quad \ldots \quad (21)$$

Where A is the area enclosed by a trap; it is the gross reservoir thickness, and N/G is the net-to-gross reservoir thickness relationship. O is the porosity, and S is the hydrocarbon saturation.

The recoverable reserve was estimated using the expression after [23]

$$R_e = (HCPV \times R_i)/F_v \quad \ldots \quad (22)$$

Where re is the recoverable reserve, Rr is the recovery factor, and Fvf is the formation volume factor. It has been generally reported that only 45% of reserves are recoverable, and 1.4 has been used as the formation volume factor in the Unam B field in the Niger Delta. In this work, the recovery factor (Rr) was taken as 45% and F_{vi}=1.4.

B. Fluid Detection

i. Gas-Bearing Formations: Gas-bearing zones were delineated where apparent density is decreased (since gas contains less dense fluids). The relationship between electron density (which is usually measured by the tool) and bulk density is somewhat different for gas than for a rock containing oil or water. The combined effect is an increase in density porosity, implying a decrease in the bulk density reading. The neutron porosity in the zone should decrease because the formation contains less hydrogen per unit volume, and the tool equates porosity with the amount of hydrogen in the formation. Hence, the combination of these two effects results in the density/neutron separation. The zone was detected with an increased resistivity response. A combination of two or more of these log behaviours was used to detect gas-bearing zones.

Published By:
Blue Eyes Intelligence Engineering and Sciences Publication (BEIESP)
© Copyright: All rights reserved.

ii. *Oil-Bearing Formations:* Oil-bearing zones were detected when the density/neutron curves tend to track together (come together), with moderate resistivity, and when the density log shows an average reading and the resistivity log shows a much lower reading than in gas-bearing zones. Hydrogen ions in oil and water-bearing formations are almost the same, but the hydrogen ions in oil-bearing formations are far more resistant than in water-bearing formations. So resistivity in formations containing oil is far higher than resistivity in brine. Also, brine has little effect on the density reading, but in oil-bearing formations, the density reading is lower because brine/water is denser than oil.

iii. *Water-Bearing Formations:* Neutron porosity is calculated assuming a water-bearing limestone matrix. Since the reservoir lithology in the Niger Delta is predominantly sandstone, the sandstone-compatible scales were used for the density and/or neutron logs. In this regard, water-bearing zones were delineated where the density and neutron curves practically overlay each other (that is, an interplay) over the whole porosity range. The resistivity curve for the same zone should indicate a highly conductive zone (low resistivity). The density log records a high reading as water is denser than hydrocarbons. Observations from relevant field logs reveal responses described above in water-bearing zones. Departures between these two curves (that is, density and neutron logs overlaying each other) were used to infer that the lithology or fluid content does not correspond to that of water-bearing sand.

IV. RESULTS

A. Well-1: Well-1 has a density log and a resistivity log. But the top part of the density log for the range 1381 to 2104 meters was omitted in interpretation, as it showed unclear scaling and values up to 100g/cc, making it unrealistic with respect to lateral sand and shale deposits in the underground. Therefore, the interpretation of petrophysical studies in this range was based solely on the resistivity log. Under this depth, resistivity and density logs were also added to the assessment. The resistivity values are very high, as recorded in the 1384-to-2095-meter reservoir, soaring to 3106 ohm-m at 1854 meters and 1080 ohm-m at 6410 meters. Such high resistivity measurements are arguably attributable to the presence of gas rather than to under-compaction, as this is deemed unlikely at a depth of approximately 2000 meters. At around 2137 meters, resistivity decreases to approximately 1.52 ohm-m, indicating a shale layer. The formations demonstrated a strongly resistive nature between 3441 and 3820 m; however, the values are lower than those in the upper reservoir section. The density log above about 2104 meters was considered unreliable, and it was reported that the unreliability may have been due to calibration problems, with the density readings being abnormally low due to gas effects. Below 2104 m, the density is typical of the usual variations within sand and shale sequences as recorded in the density log. Remarkably, density values are absent between 3085 and 3088 meters, which could be due to instrument malfunction or to a period when logging runs were not combined (Fig. 4).

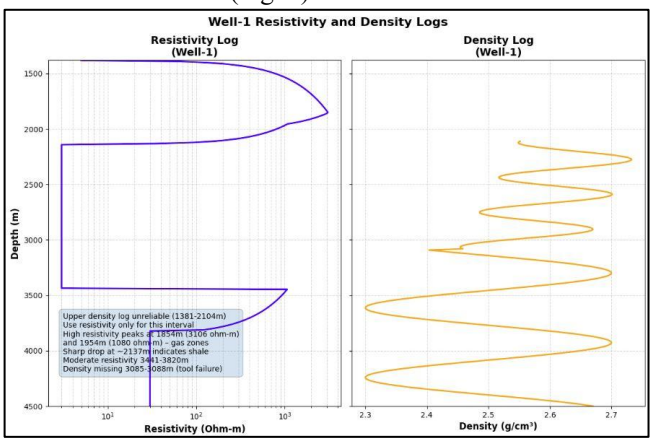

[Fig.4: Resistivity and Density Logs of Well 1]

B. Well-2: Well-2 has gamma-ray, resistivity, and density logs. Figure 1 shows that, at the logging interval, a thick shale formation extends from 3091 to 3845 meters, with sand streaks at 3835-3838 m, 3585-3600 m, 3522-3529 m, and 3225-3227 m. The support from the density log comes from high-density values, indicating thick shale. In the range of 1851 to 3070 meters, there is alternation of sand and shale, and above them is thick sand which records very high resistivity values, especially right up to about 2155 meters. These high resistivity values indicate the possibility of gas. Reservoirs within the range of 2229 to 2494 meters exhibit middle resistivity, which suggests the presence of liquid hydrocarbons, although the density log through this section shows low sand values as compared to an average seen throughout the logged area, indicating that the liquid hydrocarbons may be the condensate. The density log shows a compaction pattern typical throughout the depth range; density increases with depth (Fig. 5).

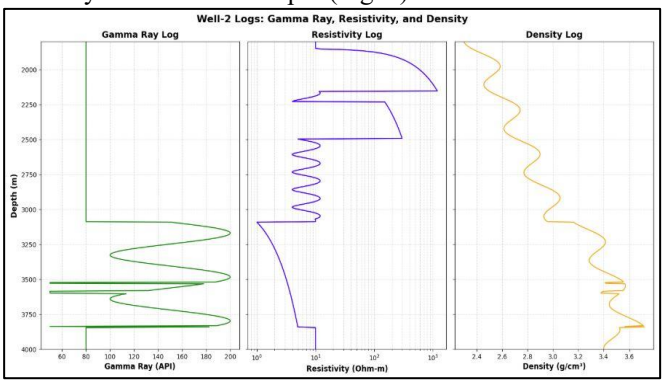

[Fig.5: Gamma Ray, Resistivity, and Density Logs of Well 2]

C. Well-3: Like Well-2, Well-3 has gamma ray, resistivity, and density logs. The upper one, at 1052-1720m, is composed of sand with extremely high resistivity and low density. At around 1524 meters, no data on gamma rays and density are present. The reservoirs lying between 2983-3073 meters and 3190-3204 meters show very

Retrieval Number: 100.1/ijies.B120915020126
DOI: 10.35940/ijies.B1209.12121225
Journal Website: www.ijies.org

Published By:
Blue Eyes Intelligence Engineering and Sciences Publication (BEIESP)
© Copyright: All rights reserved.

high resistivity levels that are almost identical to the top sand's reservoir level, implying the presence of gas. The first tank (2983 3073 m) has a clear gas-water contact, most of the first half of the reservoir has very low resistivity, and at the top is a high resistivity zone. Moreover, very low-density values are observed in this reservoir, and they are clipped due to the plotting scale. In Well-3, these low-density zones in the two reservoirs are the only ones, with density typically increasing with depth (Fig. 6).

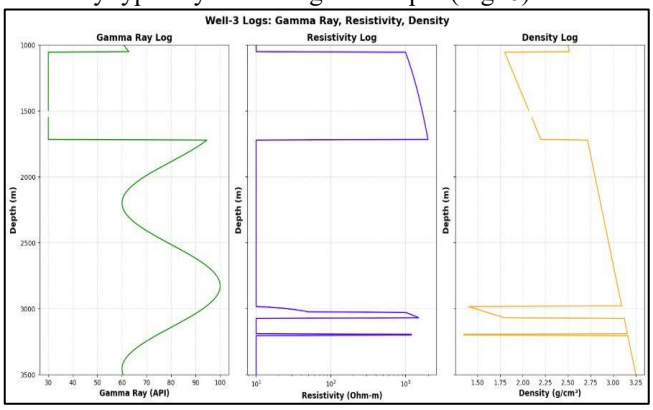

[Fig 6: Gamma Ray Resistivity and Density Logs of Well 3]

D. Well-4: Well-4 has gamma ray and neutron logs. Porosity for this well was read directly from the log and corrected for gas and shale effects. The top and bottom of the well have thick sand with little shale intercalations. Their neutron porosity tools' readings were also low. In the upper part, 1277-1716 m, the neutron log has no data (Fig. 7).

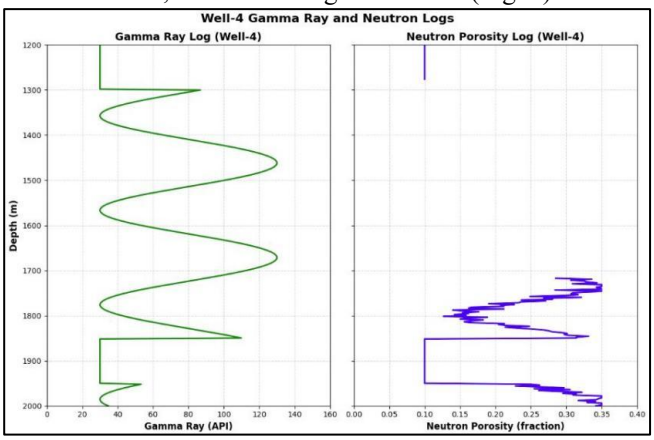

[Fig.7: Gamma Ray and Neutron Logs of Well 4]

E. Well-5: Well-5 has resistivity, density, and neutron logs, and the upper part of the sand reservoir of this well shows high values of resistivity, just as in the other wells. The density logs show a normal compaction trend: it increases with depth. An average porosity, estimated from both the density and neutron logs, was used to provide porosity measurements for this well. Figures 11 through 15 show the information about the well log data. Based on these logs, the lithologies interpreted are mostly sand and shale layering that dominate the Agbada Formation. Table 3 presents the reservoirs observed in all wells, referred to as sands 1 to 16 simply for convenience, and the results of the petrophysical analysis. Both wells had relatively continuous, highly permeable sand formations of thick nature down to a depth of 7010 feet (2137 meters) in Well-2 and 6770 feet (2064 meters) in Well-5, as shown in Table 4 and Fig. 8.

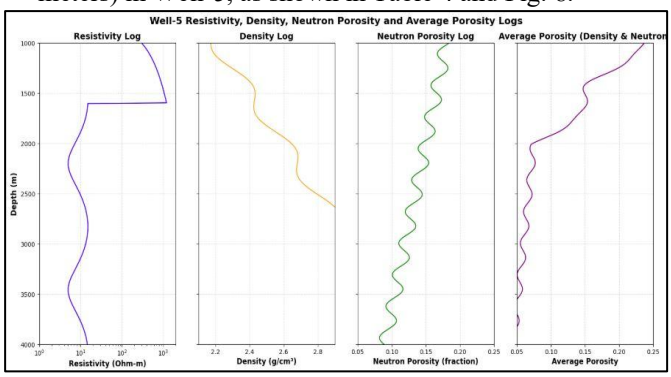

Fig 8: Resistivity, Neutron, Porosity, and Average Logs

The field consists predominantly of numerous thin sand beds, displaying irregular and warped extents across wells, with significant thickness variation between wells. Sixteen reservoirs (S1–S16) are identified, distributed unevenly: fifteen in Well-2, fourteen each in Wells 1 and 4, thirteen in Well-5, and twelve in Well-3. Hydrocarbon column limits are defined by contacts such as gas-water (GWC), gas-oil (GOC), oil-water (OWC), gas-down-to-shale (GDT), and oil-down-to-shale (ODT). Porosity ranges from about 20% in S14 (Well-1) and S13 (Well-3) to 32% in the upper sections of Wells 1 and 4, generally decreasing with depth. Permeability varies widely, from as low as 7 mD in S8 (Well-1) and S14 (Well-4) to as high as 781 mD in S1 (Well-1), strongly influenced by shale volume (Vsh) rather than depth. Some reservoirs, such as S12, S14, S15, and S16, are absent (pinched-out) in specific wells due to changes in sediment supply or transport energy. Water saturation ranges from 13% to 98%, with net-to-gross ratios from 1.0 to 0.36, underscoring reservoir heterogeneity (Fig. 9).

Reservoir thickness and net sand thickness positively influence hydrocarbon accumulation, while low shale volume (Vsh < 0.3) indicates good reservoir quality. Optimal porosity supports storage and flow, with water saturation (Sw) below 0.5 suggesting hydrocarbon presence. Permeability (K) enables hydrocarbon flow. Fluid contacts like GWC, GOC, GDT, and ODT mark hydrocarbon zones, whereas wet zones indicate water saturation or non-pay intervals. Hydrocarbon pore volume (HCPV) quantifies the volume of hydrocarbons within a pore. Sands with these markers and significant hydrocarbons are interpreted as pay zones. Thickness and fluid types assist in vertical and lateral reservoir delineation. For example, Sand 1 in Wells 1–5 shows large hydrocarbon volumes and contact markers, whereas zones labelled "Wet" typically indicate non-pay intervals (Table 4).

Published By:
Blue Eyes Intelligence Engineering and Sciences Publication (BEIESP)
© Copyright: All rights reserved.

Table IV: Results of Petrophysical Analysis of Sands S1 to S16 of the Study Area

Sand	Well	Sand Interval	Sand Interval	Reservoir Thickness		V_{sh}	φ	F	S_w	K	Fluid	Remark	HCPV
1	1	4540-6870	1384-2095	711	698	0.10	32	8	23	781	1796	GWC	
	2	4580-7010	1396-2137	741	670	0.05	29	9	21	666	1915	GDT	
	3	3460-6680	1055-2037	982	830	0.09	31	8	26	687	1723	GOC	663824.7 barrel of oil + 1312227 Scf of gas
	4	4195-6710	1279-2046	767	665	0.11	32	8		688	1954	GEC	
	5	5610-6770	1710-2064	354	311	0.09	31	8	21	687	2061	GDT	
2	1	7050-7080	2149-2159	10	10	0.39	30	9	98	12	Wet	Wet	
	2	7070-7150	2155-2180	25	22	0.37	29	9	30	12	Wet	Wet	
	3	6980-7100	2128-2165	37	33	0.36	29	9	68	13	Wet	Wet	499149 Scf of gas
	4	6950-7110	2119-2168	49	39	0.38	30	9		13	Wet	Wet	
	5	6790-7050	2070-2149	79	60	0.33	28	10	33	14	2085	GWC	
3	1	7340-7580	2238-2311	73	53	0.20	30	9	64	131	Wet	Sh	
	2	7329-7770	2232-2369	137	89	0.12	30	9	36	360	Wet	GWC	
	3	7570-7900	2308-2409	101	76	0.14	30	9	33	280	2348	Wet	106293.6 Scf of gas
	4	7320-7880	2232-2402	170	51	0.71	12	14		10	Sh	GWC	
	5	7250-7430	2210-2265	55	41	0.25	27	11	23	30	2244	GWC	
4	1	7880-8070	2402-2460	58	46	0.30	31	8	76	48	Wet	Wet	
	2	7830-8070	2387-2460	73	61	0.12	30	9	25	360	2430	GWC	
	3	7940-8060	2421-2457	36	32	0.23	28	10	58	51	Wet	Wet	612521.8.9 Scf of gas
	4	7900-7990	2409-2436	27	12	0.16	29	9		147	2427	GWC	
	5	7820-8100	2384-2470	86	49	0.12	27	11	43	154	2463	GWC	
5	1	8160-8290	2488-2527	39	29	0.17	29	9	21	145	2500	GOC	
	2	8150-8220	2485-2506	21	29	0.25	27	11	19	30	2500	ODT	1889930 barrel of oil + 4187172 Scf of gas
	3	8100-8170	2470-2492	21	16	0.24	30	9	23	79	2488	ODT	
	4	8100-8180	2470-2494	24	21	0.15	29	9		187	Wet	Wet	
	5	8160-8340	2486-2543	57	50	0.16	28	10	35	124	2521	GWC	
6	1	---	---	---	---	----	---	---	---	---	---	---	
	2	8330-8400	2540-2561	21	21	0.07	28	10	21	390	2555	GWC	37490 Scf of gas
	3	8280-8320	2524-2537	13	11	0.13	27	11	20	136	2534	GWC	
	4	8280-8340	2524-2543	19	19	0.12	26	11		114	2537	GWC	
	5	---	---	---	---	---	---	---	---	---	---	---	
7	1	8480-8700	2585-2652	67	58	0.03	28	10	73	647	Wet	Wet	
	2	8510-8650	2595-2637	42	38	0.20	28	10	23	75	2607	GWC	
	3	8440-9690	2573-2649	76	40	0.20	26	11	38	41	2622	GWC	124846.3 of Scf gas
	4	8460-8790	2579-2680	101	45	0.20	27	11		56	2619	GWC	
	5	8350-8750	2546-2668	122	72	0.10	27	11	38	199	2640	GWC	
8	1	8920-9040	2720-2756	36	30	0.39	28	10	86	7	Sh	Sh	
	2	8800-9070	2683-2765	82	36	0.30	27	11	67	16	Sh	Sh	
	3	8740-9000	2665-2744	79	38	0.24	27	11	46	34	2732	OWC	166377.8 barrel of oil + 59598 Scf of gas
	4	8850-9030	2698-2753	55	20	0.25	28	10	40	----	WET	Wet	
	5	--------	--------	----	------	-----	----	----	---	----	-----	------	
9	1	9050-9440	2759-2878	119	90	0.10	25	12	49	109	2854	GWC	18802.7 barrel of oil+74114 Scf of gas
	2	9290-9310	2832-2838	6	6	0.15	27	11	20	105	2927	GDT	
	3	9579-7900	2308-2409	101	76	0.14	30	9	33	280	2348	GWC	
	4	-------	-------	------	-----	-----	----	----	---	----	-----	-----	
	5	9320-9460	2841-2884	43	36	0.13	26	11	46	100	2866	GOC	
10	1	-------	---------	----	-----	-----	----	----	---	----	------	------	
	2	9570-9690	2918-2954	36	33	0.13	28	10	21	182	2939	GWC	90135.4 barrel for oil + 44452.3 Scf of gas
	3	9510-9630	2899-2936	37	34	0.10	25	12	22	107	2933	ODT	
	4	9550-9620	2912-2933	21	20	0.18	26	11		53	2927	GWC	
	5	-------	--------	------	-----	-----	----	----	---	----	------	-----	
11	1	9810-9950	2991-3034	43	37	0.10	26	11	84	147	Wet	Wet	
	2	9870-10070	3009-3024	61	40	0.18	26	11	32	53	3061	GWC	
	3	9810-10010	2991-3052	61	39	0.10	23	14	18	55	3049	GDT	108232.3 Scf of gas
	4	9870-10090	3009-3076	67	55	0.16	25	12		64	3076	GWC	
	5	9640-9870	2939-3009	70	43		25	12		50	Wet	Wet	
12	1	10170-10440	3101-3183	82	74	0.01	23	14	32	171	3159	GOC	

Published By:
Blue Eyes Intelligence Engineering and Sciences Publication (BEIESP)
© Copyright: All rights reserved.

	2	--------	-------	------	------	------	----	----	---	----	------	------	17631.8 barrel of oil + 65939.5 Scf of gas
	3	--------	-------	------	------	------	----	----	---	----	------	------	
	4	--------	-------	------	------	------	----	----	---	----	------	------	
	5	10090-10350	3076-3155	79	38	0.06	24	13	56	128	3116	GOC	
13	1	10490-10350	3198-3271	72	60	0.32	26	11	46		3259	GDT	59685.7 Scf of gas
	2	10610-10650	3235-3247	12	12	0.31	26	11	22	10	3244	GDT	
	3	10530-10600	3210-3232	22	13	0.21	20	18	18	23	3231	GDT	
	4	10560-10640	3220-3244	24	17	0.24	24	13		13	3241	GDT	
	5	10410-10530	3174-3210	36	20	0.24	25	12	23	18	3201	GDT	
14	1	10790-11680	3290-3561	271	215	0.01	20	18	80	55		Wet	313611.9 Scf of gas
	2	11510-11530	3509-3515	6	6	0.14	26	11	19	88	3515	GOC	
	3	--------	--------	------	------	------	----	----	---	----	------	-------	
	4	11010-11830	3357-3607	250	240	0.29	24	13		7	3598	GWC	
	5	11020-11400	3360-3476	116	89	0.15	22	14	96	20	Wet	Wet	
15	1	11880-12040	3622-3671	49	40	0.01	21	17	96	82	Wet	Wet	5345.45 barrel of oil + 19600 Scf of gas
	2	11730-11800	3576-3598	22	10	0.10	25	12	44	107	3588	GOC	
	3	--------	--------	-----	-----	-----	----	----	---	----	------	------	
	4	11850-12490	3613-3808	195	190	0.20	24	13		22	Wet	Wet	
	5	11750-11910	3582-3631	49	38	0.13	23	14	98	37	Wet	Wet	
16	1	12220-12520	3726-3817	91	86	0.02	21	17	20	72	3802	GWC	114849.7 Scf of gas
	2	12540-12700	3823-3872	94	30	0.14	24	13	51	46	3860	GWC	
	3	-------	------	-----	-----	-----	----	----	---	----	-----	------	
	4	12500-12900	3811-3933	122	118	0.04	22	15	---	82	3887	GWC	
	5	12040-12680	3671-1866	195	103	0.06	22	15	86	63	Wet	Wet	

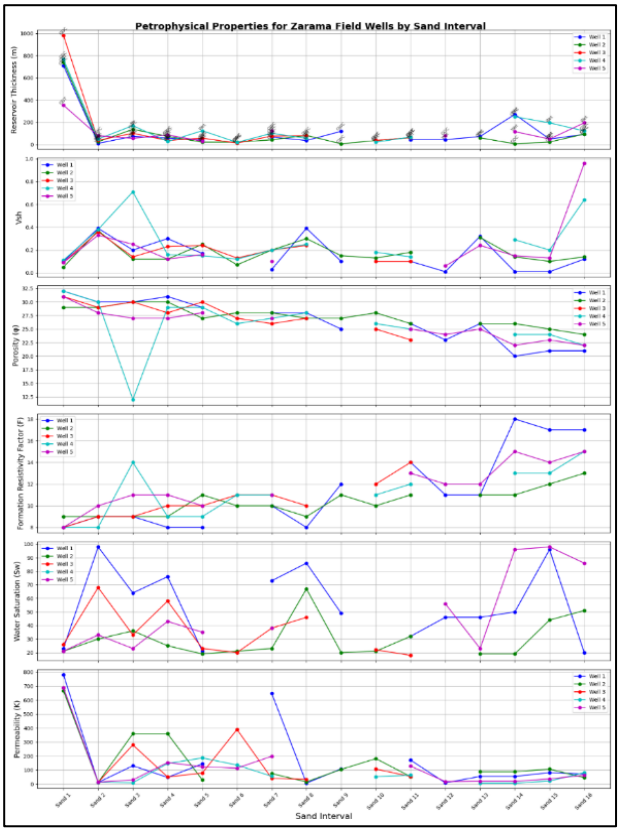

[Fig.9: Results of Petrophysical Analysis of Sands S1 to S16 of the Study Area]

The thickness of the reservoir, as determined by detailed petrophysical analysis of 16 sands in several wells, ranges from thin beds (~6 m) to thick units (>700 m), with shale volume and porosity playing a dominant role in reservoir quality. Zarama field consists mainly of gas-saturated sands having an oil/condensate gap both vertically and laterally. It should be noted that the thick, laterally extensive sands, such as S1 and S3, are porous and highly permeable, with large hydrocarbon pore volumes, which underscores their significance as reservoirs. The quality of thinner, more water-saturated reservoirs is low. Shale-bearing strata act as fluid traps or barriers, thereby affecting hydrocarbon distribution. The variations in heterogeneous petrophysical properties reflect typical Niger Delta deltaic variability, necessitating multi-well, comprehensive evaluation to ensure proper reservoir characterization and development. In general, the data suggest that the reservoir system is gas-bearing with good production potential, which is moderated by variations in lithology and fluid distribution (Fig. 10).

Retrieval Number: 100.1/ijies.B120915020126
DOI: 10.35940/ijies.B1209.12121225
Journal Website: www.ijies.org

Published By:
Blue Eyes Intelligence Engineering and Sciences Publication (BEIESP)
© Copyright: All rights reserved.

Table V: Comparison of Petrophysical Analysis in the Study Area

Property	Well	Sand															
		1	2	3	4	5	6	7	8	9	10	11	12	13	14	15	16
V_{sh}	1	0.10	0.39	0.20	0.30	0.17	-----	0.03	0.39	0.10	-----	0.10	0.01	0.32	0.01	0.01	0.12
	2	0.05	0.37	0.12	0.12	0.25	0.07	0.20	0.30	0.15	0.13	0.18	----	0.31	0.14	0.10	0.14
	3	0.09	0.36	0.14	0.23	0.24	0.13	0.20	0.24	0.14	0.10	0.10	----	0.21	----	----	----
	4	0.11	0.38	0.71	0.16	0.15	0.12	0.20	0.25	-----	0.18	0.14	----	0.24	0.20	0.20	0.64
	5	0.09	0.33	0.25	0.12	0.16	----	0.10	----	0.13	----	0.16	0.06	0.24	0.15	0.13	0.96
Porosity (φ)	1	32	30	30	31	29	----	28	28	25	-----	26	23	26	20	21	21
	2	29	29	30	30	27	28	28	27	27	28	26	----	26	26	25	24
	3	31	29	30	28	30	27	26	27	30	25	23	----	-----	-----	----	----
	4	32	30	12	29	29	26	27	28	-----	26	25	----	24	24	24	22
	5	31	28	27	27	28	----	27	----	26	----	25	24	25	22	23	22
F	1	2	9	9	8	9	----	10	10	12	----	11	14	11	18	17	17
	2	9	9	9	9	11	10	10	11	11	10	11	----	11	11	12	13
	3	8	9	9	10	9	11	11	11	9	12	14	----	18	----	----	-----
	4	8	9	14	9	9	11	11	10	-----	11	12	----	13	13	13	15
	5	2	10	11	11	10	-----	11	----	11	-----	12	13	12	15	14	15
S_w	1	23	98	64	76	21	-----	73	86	49	-----	84	32	46	50	96	20
	2	21	30	36	25	19	21	23	67	20	21	32	----	22	19	44	51
	3	26	68	33	58	23	20	38	46	33	22	18	-----	-----	-----	-----	----
	4	-----	-----	----	----	----	----	-----	40	-----	-----	-----	-----	-----	-----	-----	-----
	5	21	33	23	43	35	-----	38	-----	46	-----	-----	56	23	96	98	86
K(mD)	1	781	12	131	48	145	-----	647	7	109	-----	147	171	9	55	82	72
	2	666	12	360	360	30	-----	75	16	105	182	53	-----	10	88	107	46
	3	687	13	280	51	79	390	41	34	280	107	55	-----	23	-----	-----	-----
	4	688	13	10	147	187	136	56	-----	-----	53	64	-----	13	7	22	82
	5	687	14	30	154	124	114	199	-----	100	----	50	128	18	20	37	63

Table 5 presents a detailed petrophysical evaluation of five wells in the Zarama field, characterised by alternating sands and shales typical of the Agbada Formation, with reservoir thicknesses ranging from thin to very thick. Shale volume (Vsh) varies significantly both within and between reservoirs, greatly affecting permeability more than porosity, which generally ranges between 20% and 32%. Permeability spans a wide range from 7 mD to 781 mD and is strongly influenced by shale content. Formation resistivity factors and water saturation data reveal fluid contacts, including gas-water, gas-oil, and oil-water. Key reservoir sands like S1 and S3 demonstrate high porosity, good permeability, and substantial hydrocarbon pore volume, indicating excellent production potential dominated by gas and some oil/condensate. Despite some gaps in log data and gas-related density anomalies, integrated multi-well log analysis highlights vertical fluid presence and lateral heterogeneity, supported by shale seals. This assessment estimates recoverable hydrocarbons in millions of barrels of oil equivalent and large gas volumes, underscoring the importance of precise reservoir characterization for effective development planning.

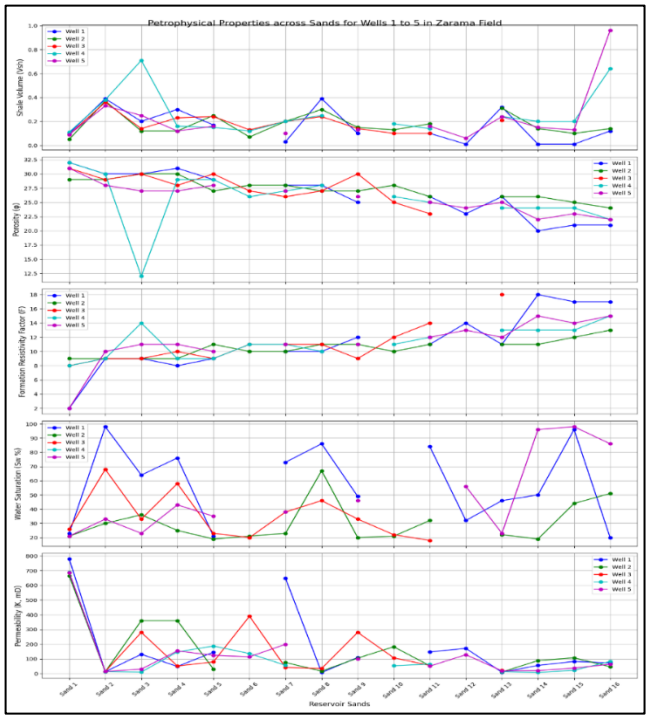

[Fig.10: Comparison of Petrophysical Analysis in the Study Area]

© Copyright: All rights reserved.

Table VI: Correlation of Reservoirs Across the Wells in the Study Area

	Well 1	Well 2	Well 3	Well4	Well 5
	Reservoir interval (m)				
S_1	1384-2095	1396-2137	1055-2037	1279-2046	1710-2064
S_2	2149-2159	2155-2180	2128-2165	219-2168	2070-2149
S_3	2218-2311	2232-2369	2308-2409	2232-2402	2210-2265
S_4	2402-2460	2387-2460	2421-2457	2409-2436	2384-2470
S_5	2488-2527	2485-2506	2470-2491	2470-2494	2486-2543
S_6	---------	2540-256	2524-2537	2524-2543	---------
S_7	2585-2652	2595-2637	2573-2649	2579-2680	2546-2668
S_8	2720-2756	2683-2765	2665-2744	2698-2753	-------
S_9	2759-2878	2832-2838	-------	--------	2841-2884
S_{10}		2918-2934	2899-2936	2912-2933	------- --
S_{11}	2991-3034	3009-3070	2991-3052	3009-3076	2939-3009
S_{12}	3101-3183	-------	--------	--------	3076-3155
S_{13}	3198-3271	3235-3247	3210-3232	3220-3244	3174-32)0
S_{14}	32.90-3561	3509-3S15	------	3357-3607	3360-3476
S_{15}	3622-3671	3576-3598	--------	3613-3808	3582-3631
S_{16}	3726-3817	3823-3872	------	3811-3900	3671-3866

Table 6 summarizes the depths of the identified reservoir sand units (S1 to S16) in six identified wells within the Zarama field. The majority of sand units (S1 to S5 and S7 to S11) exhibit good lateral continuity and are consistently similar across wells, with the depth of the juxtaposed intervals closely matching. Nevertheless, a few sands, e.g., S6, S8, S9, S12, S14, S15, and S16, are either missing or non-existent in a few wells, which means that there are vertical and lateral changes in the presence of the reservoirs, most probably because of the depositional heterogeneity or the truncation by erosion. The depth ranges also show minor differences between the wells, but generally follow the same trend as the Offshore Niger Delta Agbada Formation. This correlation trend notes that although the reservoir sands tend to be more or less continuous vertically across the field, there are regions of local sand thinning, pinch-outs, or facies evolution that are significant for mapping the reservoir correctly and for planning production (Fig. 11).

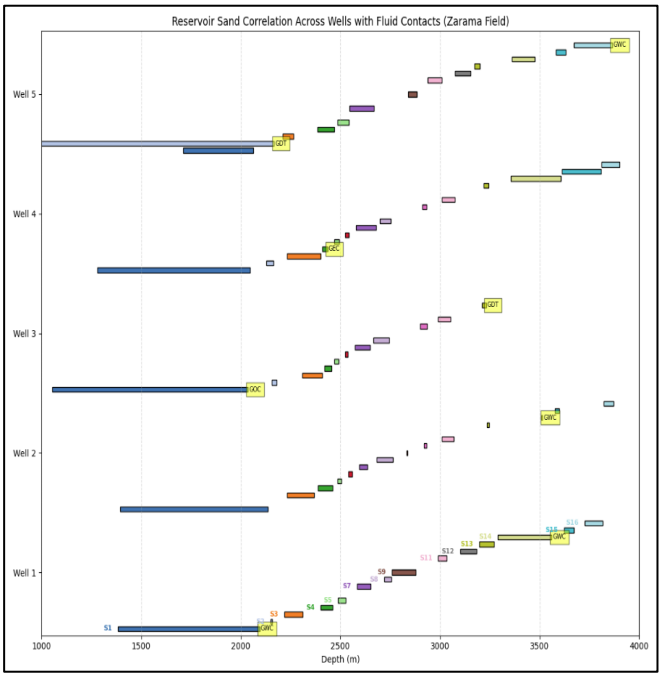

[Fig.11: Correlation of Reservoirs Across the Wells in the Study Area]

V. DISCUSSION

The reservoir of the study area, as shown by Wells 1-5, is of excellent quality, with porosity values as high as 32 per cent but generally exceeding 20 per cent. Porosity is usually found to decrease with depth, likely due to compaction, which is stronger at depth in offshore environments. Results show that although porosity has a similar average across wells, permeability exhibits significant variation due to conflicting geology and reservoir heterogeneity. Well log analysis indicates that compaction may have begun earlier in older reservoirs, as there was a substantial reduction in porosity in Wells 3 and 5 compared to Well 1. There is moderate lateral consistency in geologic and petrophysical properties, particularly permeability, across the wells. Notably, though, there is quite a wide range of permeability, from very high at 781 mD in Sand 1 (S1) of Well-1 to as low as 12 mD in Sand 2 (S2). Porosity is not the sole reason for this variability, as the volume of shale (Vsh) or shale content is also a key factor. The presence of a large volume of shale has a strong negative influence on permeability, while porosity has a positive impact, as shale is expected to destroy reservoir quality. The volumes of Shale in the eastern wells (Wells 1 and 2) are larger than those in the western wells (Wells 4 and 5), indicating that sand development increases as one moves towards Well 5 (Fig. 12).

Retrieval Number: 100.1/ijies.B120915020126
DOI: 10.35940/ijies.B1209.12121225
Journal Website: www.ijies.org

Published By:
Blue Eyes Intelligence Engineering and Sciences Publication (BEIESP)
© Copyright: All rights reserved.

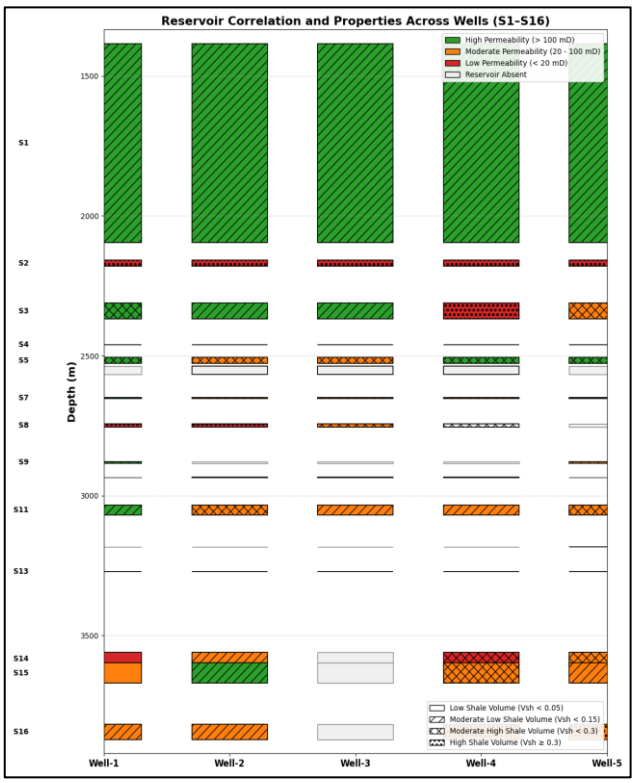

[Fig.12: Well-to-Well Reservoir Correlation in the Study Area]

Petrophysical analysis shows that porosity, permeability, and thickness exhibit minor lateral variations, with reservoir thicknesses ranging from about 6 meters to over 700 meters. Unlike other Niger Delta reports, thickness does not increase with depth; instead, shale volume increases downward. Sands S1, S3, S14, and S16 are massive and likely continuous with good structural and stratigraphic traps in deeper offshore areas. Despite lacking core samples, wireline log-derived SE petrophysical parameters strongly correlate with nearby core data, yielding accurate estimates of water saturation (Sw) and cementation factors, with cross-plot RMS errors of around 0.05. The Well-to-Well reservoir correlation visually replicates the similarities in sand zones across wells, providing a user-friendly representation of reservoir cross-sections and depth relationships. It uses colour-coded zones (pay, wet, shale) and varied sand textures to quickly identify lateral correlations and assess whether reservoir sands are continuous or heterogeneous in geometry. Well labels and depth scales allow clear visualization of stratigraphy, fluid trends, contacts, and potential pay zones. This correlation plot is crucial for reservoir characterisation, enabling geoscientists and engineers to evaluate reservoir connectivity, continuity, and geological framework, thereby aiding volume estimation, development planning, and enhanced recovery decisions. Different textures improve the distinction between strata in complex stratigraphy, enhancing reservoir management through integrated geological and petrophysical data across multiple wells (Fig. 13).

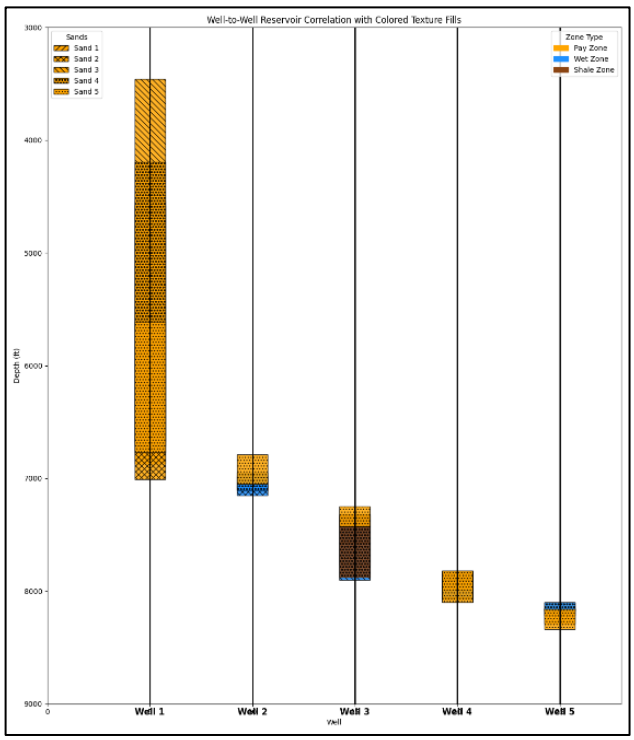

[Fig.13 (a): Well-to-Well Reservoir Correlation of the Study Area]

The sand-and-shale regime forms an alternating sequence characteristic of the Agbada Formation and depicts sixteen reservoir sands with fluctuating thicknesses and lateral discontinuities. Other main parameters of the reservoirs were calculated using known empirical models and log interpretation principles, including shale volume, porosity, permeability, and fluid saturations. The porosity ranged from 20 to 32 % and, in most cases, exhibited a decreasing trend with depth. In contrast, permeability ranged from 7 mD to 781 mD, with shale content the primary factor affecting it. High resistivity and typical density-neutron log crossovers were used as an indication of gas-bearing zones. In contrast, oil and water zones were identified based on log responses and fluid saturation. Gas-water, gas-oil, and oil-water contacts were detected, which helped map hydrocarbon columns. The findings indicate that the Zarama field is heavily saturated with gas, with oil/condensate fields, backed by thick, wide sandstones, topped with thick, laterally continuous shale caps. Although there were difficulties to address, such as poor quality of logs (density log anomalies caused by gas effects) and a few missing data gaps, the integrated log method was successful in giving and characterized reasonable estimates of hydrocarbon pore volumes and recoverable reserves, say around 2.85 million barrels of oil equivalent and close to 5.85 billion cubic feet of gas. The presence of well variations in reservoir thickness and properties is indicative of the lateral heterogeneity typical of the Niger Delta. The paper concludes that, in general, the research supports good reservoir quality and high potential for reserves, and provides a sound petrophysical basis for establishing future

Published By:
Blue Eyes Intelligence Engineering and Sciences Publication (BEIESP)
© Copyright: All rights reserved.

development and production strategies for the Zarama field (Fig. 13).

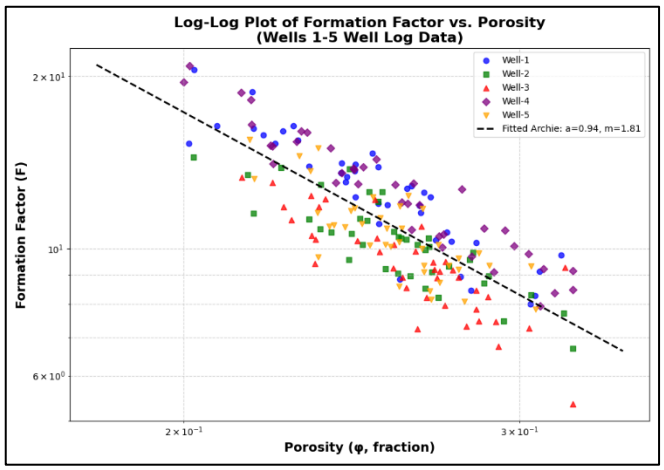

[Fig.13 (b): Log-Log Plot of Formation Factor as a Function of Porosity for the Wells Applying the Equation log(F) = Log (a) – mlog (φ)Derived from Archie's Formation Factor Equation $F=\Theta^{-m}$ to the Study Area]

The study area predominantly features gas-bearing reservoirs, as indicated by high resistivity values—especially in the thick Sand 1 (S1)—and neutron log cross-overs observed in Wells 4 and 5. Notably, even at depths near 3872 m (S16, Well-2), porosity remains high, reaching up to 24%. Some oil-charged sands, mainly condensates, appear intermittently, such as at a depth of 2900 m in Well-3. Hydrocarbon accumulation is likely linked to pre-charge events during basin subsidence and structural deformation. Petrophysical indicators, including shale volume, porosity, permeability, and gamma-ray logs, suggest generally homogeneous pay zones, mainly composed of thinly bedded sands consistent with Niger Delta patterns, in which over 70% of oil columns are under 15 m thick. Resistivity variations reflect changes in porosity, clay content, and hydrogen index, with resistivity anomalies due to clay-bound water. Hydrocarbon column thickness varies widely—Well-2's is about 6 m, whereas Well-3 may exceed 830 m, unusually thick for the Niger Delta. Thick reservoirs like S1 show gas accumulation, as suggested by resistivity and density logs, although data gaps above the seals limit confirmation. Core S13's gas-filled zones, capped by ~165 m shale, exemplify lateral structural trapping. (Fig. 12).

Hydrocarbon zones mainly occur within these depth ranges in the wells (Table 4):

Well 1: 1384–2095 m, 1396–2137 m, 1055–2037 m, 1279–2046 m, 1710–2064 m (all marked with GWC, GOC, GDT, GEC indicating hydrocarbon presence)

Well 2: The pay zone near 2070–2149 m (GWC), while upper intervals (2149–2159 m to 2119–2168 m) are wet zones.

Well 3: Mixed wet and shale zones, but pay zones around 2210–2265 m (GWC) and similar intervals.

Well 4: Hydrocarbon zones around 2387–2460 m, 2409–2436 m, 2384–2470 m with GWC, while some intervals are wet.

Well 5: Pay zones roughly 2488–2543 m, with GOC and ODT markings, generally hydrocarbon bearing.

The general findings on reservoir quality, variability, petrophysical controls, reservoir architecture, the presence of hydrocarbons, and the implications of production in the study area Wells 1-5.

VI. CONCLUSION

Characteristic description of the reservoir property of the study region consists of Wells 1 to 5, a perfect quality reservoir with porosity level in the range of high up to 32 percent, with the overall average above 20 percent, showing a general pattern to decrease with depth, probably because of compactation effects in that offshore location. Although average porosity between wells is similar, permeability exhibits strong lateral and vertical gradients, ranging from very high (781 mD in Sand 1 of Well 1) to very low values, and it is primarily influenced by the extent of shale volume, which is detrimental to permeability and reservoir quality. The structural and stratigraphic trapping of heterogeneous but predominantly gas-bearing reservoir sands is confirmed by petrophysical analysis, which is also supported by the lateral continuity in the level of well-to-well correlation, which visually represents correlated pay, wet, and shale zones, aiding in defining the reservoir architecture and fluid distribution. Zone-bearing hydrocarbons are mainly located in depth ranges between 1055m and 2543m across wells, as supported by cross-plot analysis and fluid saturation factors, which highlight contact points at the GWC, GOC, and GDT. The reservoir contains a combination of thick and thin sand layers, with a wide range of shale and abundant fluids, including gas and some oil condensates. The combined petrophysical statistics indicate a non-homogeneous yet gas-bearing reservoir complex with a strong production prospect. Deviation in petrophysical properties between wells supports the need for multi-well, combined evaluation methodologies to provide an optimal strategy for reservoir characterisation and development mechanisms. Although petrophysical heterogeneity requires an integrated multi-well assessment, the result indicates a high hydrocarbon prospect with a recovery volume of up to 2.85 million barrels of oil equivalent and almost 5.85 billion cubic feet of gas. This multifaceted study, in the background of strategic reservoir management and development planning, provides the best production optimisation for the offshore reservoir in a complex, highly structural, and stratigraphic setting.

DECLARATION STATEMENT

As the article's author, I must verify the accuracy of the following information after aggregating input from all authors.

- **Conflicts of Interest/ Competing Interests:** Based on my understanding, this article has no conflicts of interest.
- **Funding Support:** This article has not been funded by any organizations or agencies. This independence ensures that the research is conducted objectively and without external influence.

© Copyright: All rights reserved.

- **Ethical Approval and Consent to Participate:** The content of this article does not necessitate ethical approval or consent to participate with supporting documentation.
- **Data Access Statement and Material Availability:** The adequate resources of this article are publicly accessible.
- **Author's Contributions:** The authorship of this article is contributed equally to all participating individuals.

REFERENCES

1. Annan Boah Evans, Aidoo Borsah Abraham1 and Brantson Eric Thompson. (2019): Integrated Reservoir Characterisation for Petrophysical Flow Units Evaluation and Performance Prediction. The Open Chemical Engineering Journal. 2019, *13*, 97-113. DOI: https://doi.org/10.2174/1874123101913010097
2. Ahmad Afshar, Maysam Abedi, Gholam-Hossain Norouzi, Mohammad-Ali Riahi. (2015): Geophysical investigation of underground water content zones using electrical resistivity tomography and ground penetrating radar: A case study in Hesarak-Karaj, Iran. Engineering Geology. Volume 196, 28 September 2015, Pages 183-193. DOI: https://doi.org/10.1016/j.enggeo.2015.07.022
3. Mehdi Saffari and Pooria Kianoush (2025): Integrated petrophysical evaluation of Sarvak, Gadvan, and Fahliyan formations in the Zagros Area: insights into reservoir characterization and hydrocarbon potential. Journal of Petroleum Exploration and Production Technology (2025) 15:54. DOI: https://doi.org/10.1007/s13202-025-01953-5
4. Orji O., Egwuonwu, G. Ndubuisi and Okpara, A. Obiora. (2024): Petrophysical Property Evaluation and Reservoir Characterization in The B-Field, Niger Delta. Journal of Basic Physical Research ISSN: 2141-8403 Prints, 2141-8411 Online Vol. 12, Issue 2, October 2024, pp. 77 - 88. Available online at https://journals.unizik.edu.ng/jbpr/
5. Mehdi Saffari and Pooria Kianoush (2025): Integrated petrophysical evaluation of Sarvak, Gadvan, and Fahliyan formations in the Zagros Area: insights into reservoir characterization and hydrocarbon potential. Journal of Petroleum Exploration and Production Technology (2025) 15:54. DOI: https://doi.org/10.1007/s13202-025-01953-5
6. Naiem Souilam Sobih, Ahmed Ahmed El Nagar, Ali Elsayed Abbas1 and Samir Shehab (2025): Integrating petrophysical characterization and reservoir evaluation of the Kafr ELSheikh formation in Sapphire field, Nile Delta, Egypt. Scientific Reports | (2025) 15:4555 | DOI: https://doi.org/10.1038/s41598-025-88056-7
7. Hina Ahmed and Manahil Sameer. (2024): Geological Analysis and Subsurface Characterization Through Well-Log Analysis: Insights into Reservoir Evaluation and Petrophysical Properties https://www.researchgate.net/publication/384920379. DOI: https://doi.org/10.13140/RG.2.2.11679.98726
8. Kii B. L., Amakiri A. R. C., Tamunoberetonari I., Sigalo F. B. (2024): Petrophysical Evaluation of Reservoir Rocks, using Well-Logs Data in Field 'DL' of the Onshore Northern Depobelt Niger Delta, Nigeria. Journal of Scientific and Engineering Research, 2024, 11(1):136-145 Research Article ISSN: 2394-2630 CODEN(USA): JSERBR. Journal of Scientific and Engineering Research, 2024, 11(1):136-145. https://jsaer.com/download/vol-11-iss-1-2024/JSAER2024-11-1-136-145.pdf
9. Kai Zhang 1, Shengqing Li, Yuanda Su, Baohai Tan 1 and Bo Zhang. (2022): Design of an Acoustic Through-Casing Logging Tool. Sensors 2022, 22, 8404. https://www.mdpi.com/journal/sensors DOI: https://doi.org/10.3390/s22218404
10. J.-L. Mari, C. Vergniault, F. Coppens. (2018): Acoustic logging. Commons License CC-BY-NC-ND allowing non-commercial use, distribution, and reproduction of the text, via any medium, provided the source is cited. © EDP Sciences, 2018 DOI: https://doi.org/10.1051/978-2-7598-2263-8.c005
11. Godwin Omokenu Emujakporue. (2016): Assessment of Hydrocarbon Potential in Owem Field in the Niger Delta, Nigeria. International Journal of Geoscience, Vol. 7, No. 3. DOI: https://doi.org/10.4236/ijg.2016.73026
12. Jin Lai, Yang Su, Lu Xia, Fei Zhao, Tianyu Bai, Yuhang Li, Hongbin Li, Yuyue Huang, Guiwen Wang and Ziqiang Qin. (2024): Application of geophysical well logs in solving geologic issues: Past, present and prospects. Geoscience Frontiers, Vol 15, Issue 3. DOI: https://doi.org/10.1016/j.gsf.2024.101779
13. Coker, J.O., Idris, J.M., Ojo, O.F., Ikhane, P.R. and Makinde, G. (2021): Application of Well Log Analysis in Assessment of Petrophysical Parameters of the Alpha Oilfield in the Niger Delta, Nigeria. IOSR Journal of Applied Geology and Geophysics (IOSR-JAGG) e-ISSN: 2321–0990, p-ISSN: 2321–0982.Volume 9, Issue 1 Ser. I, PP 39-49 https://www.iosrjournals.org/iosr-jagg/papers/Vol.%209%20Issue%201/Series-1/E0901013949.pdf
14. Wakeel Hussain, Nafees Ali, Rakhshanda Sadaf, Chuanyu Hu, Edwin E. Nykilla, Arif Ullah, Sayed Muhammad Iqbal, Altaf Hussain, and Sadam Hussain. (2022): Petrophysical analysis and hydrocarbon potential of the lower Cretaceous Yageliemu Formation in Yakela gas condensate field, Kuqa Depression of Tarim Basin, China.Geosystems and Geoenvironment Volume 1, Issue 4, November 2022, 100106. DOI: https://doi.org/10.1016/j.geogeo.2022.100106
15. Damilare S Adepehin, Fredrick F Magi, Abimbola I Odudu, Moromoke O Adelayi, and Kennedy Suleiman. (2022): Shale Volume Effect on Hydrocarbon Prospectivity of Green Field, Niger Delta, Nigeria. PHYSICSAccess Research Paper ISSN Online: 2756-3898, ISSN Print: 2714-500X. DOI: https://doi.org/10.47514/phyaccess.2022.2.1.006
16. Vianney M. Kamayou, Chukwuemeka N. Ehirim, Sunday S. Ikiensikimama. (2021): Estimating Volume of Shale in a Clastic Niger Delta Reservoir from Well Logs: A Comparative Study. International Journal of Geosciences > Vol. 12 No.10, October 2021. DOI: https://doi.org/10.4236/ijg.2025.164014
17. Porosity: Petrophysics MSc Course Notes by Dr. Paul Glover. Pp 10-20. https://cyber.cse.iitk.ac.in/MD!/1L2857C/8L712414C6/petrophysics_msc-course-notes-by-paul__glover.pdf
18. Djebbar Tiab, Erle C. Donaldson. (2016): Chapter 4 - Formation Resistivity and Water Saturation. Petrophysics (Fourth Edition) Theory and Practice of Measuring Reservoir Rock and Fluid Transport Properties 2016, Pages 187-278. DOI: https://doi.org/10.1016/B978-0-12-803188-9.00004-8
19. Publisher: Society of Petroleum Engineers (SPE). Content Sub Type: Petrowiki Content. DOI: https://doi.org/10.2118/PW1066
20. Tayfun Babadagli (2017): Development of mature oil fields — A review. Journal of Petroleum Science and Engineering. Volume 57, Issues 3–4, June 2007, Pages 221-246. DOI: https://doi.org/10.1016/j.petrol.2006.10.006
21. C.E. Neuzil. (2019): Annual Review of Earth and Planetary Sciences Permeability of Clays and Shales. Annu. Rev. Earth Planet. Sci. 2019. 47:247 73. Journal of Botany 54(2):97-114. DOI: https://doi.org/10.1146/annurev-earth-053018060437
22. Elisha James Akinola, Osetoba, Olusola A.Adekeye, Olabisi Adeleye and Adekunle Sofolabo. (2023): Well Log Analysis for Depositional Environment Interpretation. https://napebulletin.org.ng/wp-content/uploads/2024/01/4-Well-Log-29-42-final.pdf
23. Johannes Homme· Edward Coltman and Holger Class. (2018): Porosity–Permeability Relations for Evolving Pore Space: A Review with a Focus on (Bio-) geochemically Altered Porous Media.Transp. Porous. Med. (2018) 124:589–629. DOI: https://doi.org/10.1007/s11242-018-1086-2

AUTHOR'S PROFILE

Mohammed Ali Garba was born in 1978 and hails from Gwoza LGA of Borno State, Nigeria. He attended the Federal University of Technology, Yola, for his first degree in Geology, graduating in 2000. He bagged his M.Sc. degree in Applied Geophysics from the same school in 2010. Also, he earned his PhD in Exploration Geophysics from Prestigious Curtin University of Technology in Perth, Western Australia, in 2018. He began lecturing at Gombe State University in 2010, where he was promoted to the rank of Associate Professor in Geophysics in 2024. Currently, he has 16 International Publications. Also, he is a former level adviser and is now the Departmental Examination Officer for the Department of Geology at Gombe State University. A reviewer of Scientific Journals, amongst which are the Asian Journal of Geographic Research and the Bima Journal of Science. He is also an External Examiner at the Department of Geology in Adamawa State University. He has attended both local and international conferences and is also a member of various university committees and professional bodies, including ASEG, COMEG, NAPE, and NMGS.

Published By:
Blue Eyes Intelligence Engineering and Sciences Publication (BEIESP)
© Copyright: All rights reserved.

Mustapha Ali Garba was born in 1983 and hails from Gwoza LGA in Borno State, Nigeria. He attended Gadamayo Primary School in Gwoza and obtained the First Leaving Certificate in 1985. He then attended Government Day Senior Secondary School, Gwoza, and obtained his SSCE in 1991. He later attended the University of Maiduguri to pursue a First Degree in Physics in 2020. And a Postgraduate Diploma in Physics from Bayero University, Kano, Nigeria, in 2022. He bagged his M.Sc. degree in Physics from the University of Maiduguri in 2024. He started teaching at Government Day Senior Secondary School, Gwoza, in 2021. Currently, he has 2 International Publications.

Disclaimer/Publisher's Note: The statements, opinions and data contained in all publications are solely those of the individual author(s) and contributor(s) and not of the Blue Eyes Intelligence Engineering and Sciences Publication (BEIESP)/ journal and/or the editor(s). The Blue Eyes Intelligence Engineering and Sciences Publication (BEIESP) and/or the editor(s) disclaim responsibility for any injury to people or property resulting from any ideas, methods, instructions, or products referred to in the content.

© Copyright: All rights reserved.